THE ASTROPHYSICAL JOURNAL, 318:913–925, 1987 July 15

SOLAR NEUTRON EMISSIVITY DURING THE LARGE FLARE ON 1982 JUNE 3

E. L. CHUPP,[1] H. DEBRUNNER,[2] E. FLÜCKIGER,[2] D. J. FORREST,[1] F. GOLLIEZ,[2] G. KANBACH,[3]
W. T. VESTRAND,[1] J. COOPER,[3] and G. SHARE[4]
Received 1986 August 6; accepted 1987 January 6

ABSTRACT

Observations made with the gamma-ray spectrometer (GRS) on the *Solar Maximum Mission* (*SMM*) satellite and with the Jungfraujoch neutron monitor are used to determine the directional solar neutron emissivity spectrum from ~100 MeV to ~2 GeV during the solar flare on 1982 June 3. The experimental data require a time-extended emission of the neutrons at the Sun with the majority of the neutrons produced after the impulsive phase. Fits to the observational data are provided by neutron emissivity spectra with spectral forms $E_n^{-2.4}$ and $E_n^{3/8} \exp[-(E_n/0.016)^{1/4}]$. The power-law form requires a truncation at energy E_c, where 2 GeV $< E_c <$ 4 GeV. In both cases the integrated neutron emissivity for energies greater than 100 MeV is $\sim 8 \times 10^{28}$ neutrons sr^{-1}. These high-energy spectra are in agreement with the neutron spectrum for energies less than 100 MeV derived from observations of neutron decay protons. The observations also require that the first GeV protons producing the GeV neutrons interacted at the Sun within a time span of at most 16 s implying neutron production at densities $n > 10^{14}$ cm^{-3}. We have also considered the observational effects of high-energy neutron spectral changes throughout this event. The present analysis of the neutron data for $E_n \geq 100$ MeV is unable to differentiate between isotropic and nonisotropic emission of the neutrons.

Subject headings: cosmic rays: general — Sun: flares

Dedication.—The major impetus for initiating the study of high-energy solar neutrons is due to Professor Ludwig Biermann, who pointed out, in 1951, their importance in investigating the properties of the GeV protons known at that time to be produced in solar flares. The actual accomplishment of the study of solar flare neutrons was first made from the *Solar Maximum Mission* spacecraft, which was repaired in orbit by the crew of *Challenger* on mission 41-C. The pilot for that mission, and the commander of *Challenger*'s last mission, was Francis R. Scobee. This work is dedicated posthumously to the memory of these two men.

I. INTRODUCTION

Shortly after the first reports of ground-level cosmic-ray intensity enhancements (GLEs) following solar flares, Biermann, Haxel, and Schluter (1951) pointed out that the GeV protons accelerated at the Sun could produce a sufficient flux of neutrons to be observable at the Earth. These neutral radiations could, therefore, be a powerful, direct probe of solar flare particle acceleration processes, since they are not affected by the solar and interplanetary magnetic fields. In particular, measurement of the arrival time and of the energies of the neutrons could permit a detailed study of the acceleration process and spectral characteristics of the charged particles accelerated in the flare. Using the assumption that neutrons are released in a δ-function in time at the Sun, numerous calculations giving the neutron flux at the Earth have been carried out by several authors (Lingenfelter *et al.* 1965; Lingenfelter and Ramaty 1967; Ramaty, Kozlovsky, and Lingenfelter 1975; Ramaty *et al.* 1983; Murphy 1985; Kocharov and Mandzhavidze 1985) and recently Murphy and Ramaty (1985) considered finite duration of the production of neutrons at the Sun. Alsmiller and Boughner (1968) calculated the secondary neutron flux for energies less than 20 MeV at various depths in the Earth's atmosphere, expected for a burst of solar neutrons arriving at the Earth, applicable only for balloon and aircraft altitudes. Also, Roelof (1966) has examined the possibility of detecting solar neutron-decay protons accompanying primary protons from a pulse-type solar flare. However, all attempts to detect solar neutrons at the Earth and in interplanetary space were unsuccessful (Forrest and Chupp 1969; Chupp 1971; Kirsch 1973) until the observations made with the GRS on the *SMM* satellite.

The first detection of ~400 MeV solar neutrons near the Earth, following an impulsive solar flare on 1980 June 21 (Chupp *et al.* 1982), initiated an opportunity to study the highest energy particles accelerated in solar flares. A second observation of solar neutrons by the *SMM* GRS was made on 1982 June 3. During this event the interaction of solar neutrons with the Earth's atmosphere was also detected by ground-level neutron monitors (Debrunner *et al.* 1983; Efimov, Kocharov, and Kudela 1983). For three events, solar neutron decay protons have been observed near the Earth by Evenson, Meyer, and Pyle (1983) and Evenson, Kroeger, and Meyer (1985). Also, the existence of neutrons at the Sun, producing the *n-p* capture γ-ray line at 2.223 MeV, have been reported for several events (Chupp 1982; Share *et al.* 1982; Prince *et al.* 1983). It is significant that all observational methods described above are sensitive to different parts of the solar neutron spectrum. Therefore, by combining the techniques, it is possible to study the solar neutron energy spectrum over a range of energies from ~1 MeV to several GeV. As emphasized by Ramaty *et al.* (1983), this allows us to investigate the time history of particle acceleration in solar flares and to determine the total number and the energy spectrum of the accelerated ions up to

[1] University of New Hampshire.
[2] Physikalisches Institut der Universität Bern.
[3] Max-Planck Institut für Extraterrestrische Physik.
[4] E. O. Hulburt Center for Space Research, Naval Research Laboratory.

the highest energies. A study of the highest energy neutrons provides the only means of deducing the spectrum of the accelerated particles producing nuclear interactions at the Sun.

In this paper we report on the interpretation of detailed observations of solar neutrons made with the *SMM* GRS and the Jungfraujoch neutron monitor during the impulsive 1982 June 3 solar flare. Assuming that the time history of the neutron production at the Sun follows the pion production time profile, we investigate several fundamental aspects of solar particle acceleration, including (1) a determination of the integral and the differential neutron energy spectra at the Sun emitted toward the Earth, which are consistent with the total *SMM* GRS and Jungfraujoch neutron monitor data set, (2) a test for the highest energy neutrons required by the observations and evidence for a physical upper limit to the highest energy particles accelerated in the flare, (3) a determination of the time scale of the highest energy accelerated particle interactions, and (4) a consideration of the observational effects of the time evolution of the neutron spectrum at the Sun. We also compare the resulting spectra with the neutron spectral values deduced from the neutron decay protons. Finally, we explore the implications of our analysis on the basic model-independent properties of accelerated protons and ions. In the following, we, first, review the observations, second, define the method of analysis, and, third, discuss the results.

II. OBSERVATIONS

On 1982 June 3 at 1141 UT an X8/2B white light flare was produced in McMath Region 3763 (SO9E72)[5] with associated emissions from meter radio wave to γ-rays. Cosmic-ray detectors on the *Helios 1* spacecraft recorded prompt electrons of energies up to 1 MeV and protons up to 200 MeV (McDonald and Van Hollebeke 1985). *Helios 1* was at 0.57 AU from the Sun and at an angle of 120° east of the Sun-Earth direction. *IMP 8* and *ISEE 3* detectors observed protons (>10 MeV) and electrons (5–11 MeV) near the Earth (Evenson *et al.* 1984), and the *ISEE 3* also recorded energetic photons over 10 keV (Kane 1982). The GRS (Forrest *et al.* 1980) on board the *SMM*, which was in a low Earth orbit, recorded an intense solar γ-ray line event, beginning at ~1143 UT, followed by a signal characteristic of the arrival of high-energy γ rays (>10 MeV) and solar neutrons at the Earth. In near time coincidence with this event the neutron monitors at Jungfraujoch (geographic coordinates, 46°.5 N, 8°.0 E; altitude, 3554 m), Lomnicky Stit (49°.2 N, 20°.2 E; 2632 m) and Rome (41°.9 N, 12°.5 E; 60 m) registered significant increases over their normal count rates, ranging from 2.9 σ to 8.5 σ, during the time interval (1145–1150) UT (see Table 1).

In Figure 1 we show the *SMM* GRS count rate time history in several energy-loss channels and the relative excess count rate of the Jungfraujoch neutron monitor. The curve for 56–199 keV X-rays is due predominantly to electron bremsstrahlung. The curve for the 4.1–6.4 MeV photons results mainly from narrow and unresolved γ-ray lines indicative of ion interactions at the Sun. The energy-loss range greater than 25 MeV responds to high-energy neutral radiation (photons and/or neutrons) (Forrest *et al.* 1980). The relative excess count rate measured by the Jungfraujoch neutron monitor for 1 minute intervals is expressed in percent of the average count rate determined from the two $\frac{1}{2}$ hr reference intervals 1110–1140 UT and 1200–1230 UT. The neutron monitor measures the intensity of the galactic and solar cosmic radiation, incident on the atmosphere, by recording slow neutrons produced locally in the detector by the secondary nucleon cascades of the primary radiation (Simpson and Uretz 1953).

Starting with the first impulse of the flare, from ~1143–1144 UT, there is good correlation of the main features in the *SMM* GRS 56–199 keV X-ray band and 4.1–6.4 MeV γ-ray channels which continues throughout the event. For the first pulse of intense emission there is also good time correlation between the high-energy channels (>25 MeV) and the lower energy channels. At later times (>1144 UT), however, this excess count rate (>25 MeV) remains anomalously high until ~1204 UT (satellite sunset) and with a time structure not matching that at lower energies. As we discuss later, a portion of this excess high-energy count rate (>25 MeV) is due to the arrival of high-energy neutrons at *SMM*. Beginning with the time interval 1144–1145 UT, the Jungfraujoch neutron monitor count rate shows a statistically significant enhancement over the average rate until ~1155 UT which reaches a maximum of ~5% in the 1 minute averages. The six individual records in the interval 1144–1150 UT were increased at a significance

[5] *Solar Geophysical Data.* 1982, No. 455, Part 1.

TABLE 1

COSMIC-RAY NEUTRON MONITOR OBSERVATIONS OF THE SOLAR NEUTRON EVENT ON 1982 JUNE 3
(5 minute values)

	Jungfraujoch	Lomnicky Stit	Rome	Kiel
Geographic coordinates	46°.5 N 8°.0 E	49°.2 N 20°.2 E	41°.9 N 12°.5 E	54°.3 N 10°.1 E
Altitude	3554 m	2632 m	60 m	54 m
Geomagnetic proton cutoff energy[a]	3.79 GeV	3.17 GeV	5.44 GeV	1.57 GeV
Atmospheric depth to Sun at 11:45 UT	742 g cm^{-2}	881 g cm^{-2}	1105 g cm^{-2}	1222 g cm^{-2}
Average count rate[b]	43,990 cts/5 minutes	136,081 cts/5 minutes	31,997 cts/5 minutes	48,570 cts/5 minutes
Excess (%):				
1140–1145 UT	0.43 ± 0.63	0.17 ± 0.33	0.89 ± 0.71	−0.36 ± 0.50
1145–1150 UT	4.21 ± 0.63	2.80 ± 0.33	2.04 ± 0.71	0.66 ± 0.50
1150–1155 UT	2.57 ± 0.63	0.21 ± 0.33	0.04 ± 0.71	0.85 ± 0.50
1155–1200 UT	0.54 ± 0.63	1.04 ± 0.33	0.70 ± 0.71	−0.42 ± 0.50
1200–1205 UT	−1.22 ± 0.63	−0.30 ± 0.33	0.85 ± 0.71	1.27 ± 0.50

[a] Based on Shea *et al.* 1983.
[b] Corrected to standard pressure of the station.

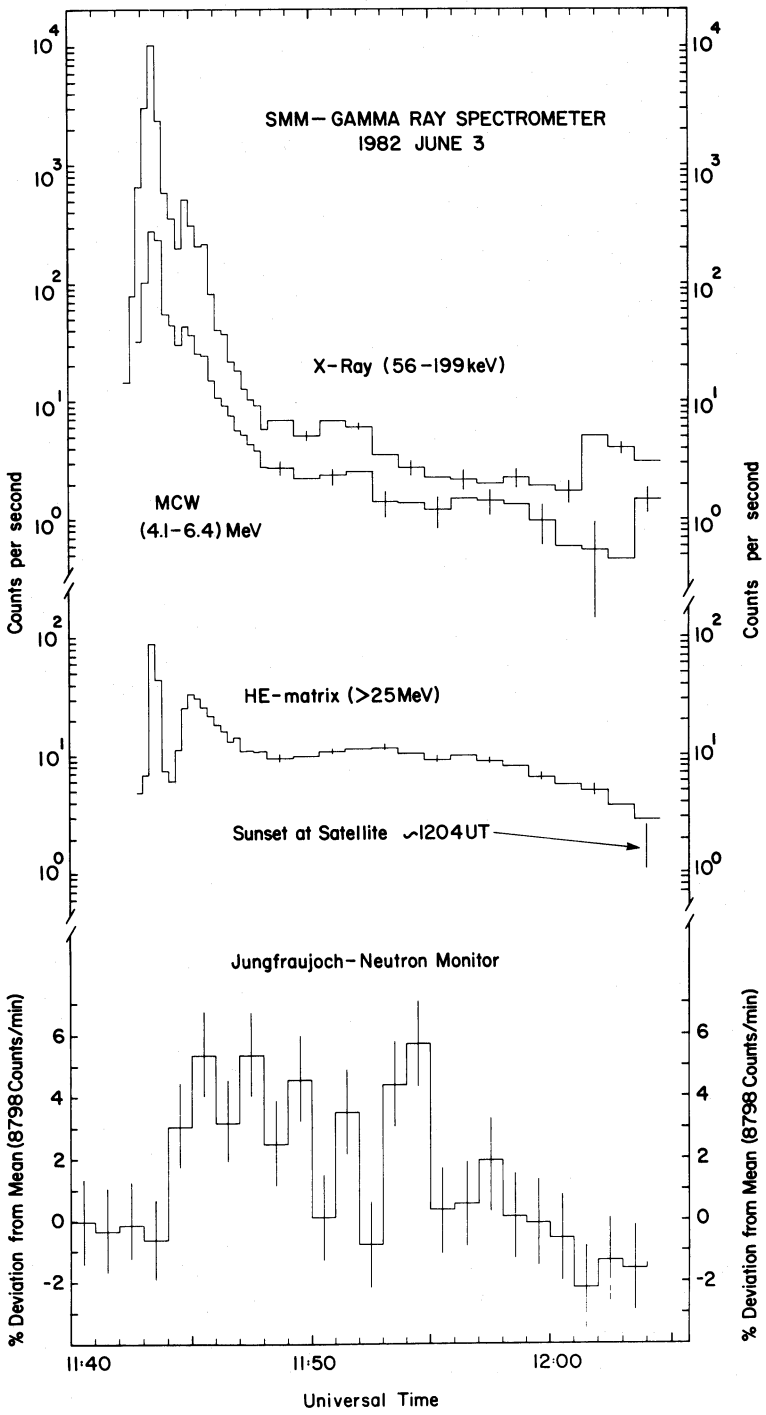

FIG. 1.—Time history for several data channels from the *SMM* GRS and for the Jungfraujoch neutron monitor count rate for the 1982 June 3 flare. Peak count rates in the GRS (X-ray) and MCW (4.1–6.4) MeV energy bands are uncertain because of pulse pile-up, excessive dead time, and photomultiplier gain shifts, and should be used with care. The highest MCW count rates have been estimated using measured live time values, averaged over 16.384 s, and a derived gain shift correction. Error bars are 1 σ based on count statistics only.

ranging from 1.8 σ to 3.9 σ, where the standard deviation was determined from the actual count rate fluctuations in the reference intervals. After 1150 UT the three count rates between 1151–1152 UT, 1153–1154 UT, and 1154–1155 UT differ by 2.6 σ, 3.2 σ, and 4.2 σ, respectively from the average count rate. In the 5 minute records the values at 1145–1150 UT and at 1150–1155 UT show enhancements of 6.7 σ and 4.1 σ, respectively, above the average count rate as shown in Table 1, column (2). Five-minute averaged count rates are also available from other neutron monitor stations. In Table 1 we list, for comparison with the records at Jungfraujoch, the measurements obtained at Lomnicky Stit, Rome, and Kiel (geographic coordinates, 54°3 N, 10°1 E; altitude, 54 m), kindly made available to us (Kudela 1983; Zangrilli 1983; Rohrs 1983). For the time interval 1150–1155 UT only the Jungfraujoch monitor at an altitude of 3554 m registered an enhanced count rate.

III. INTERPRETATION AS A SOLAR NEUTRON EVENT

Evidence that high-energy neutrons, greater than 300 MeV, were produced in the event comes from the network of cosmic-ray neutron monitor stations. As shown in Table 1 the high-altitude monitors at Jungfraujoch and Lomnicky Stit measured small but significant increases in the average 5 minute count rate in the time interval 1145–1150 UT, 6.7 σ and 8.5 σ, respectively. The Rome neutron monitor also showed a small 2.9 σ increase. The Kiel sea level neutron monitor, however, registered an *insignificant* 1.3 σ enhancement. It is noteworthy that Jungfraujoch, Lomnicky Stit, and Rome are located at mid-latitudes and that these stations observed the increase around local noon.

There is no evidence that the enhancement was produced by energetic protons since the measurements by the other stations in the worldwide network of neutron monitors showed no enhancement. Furthermore, the flare location was S09E72, making the existence of prompt solar protons near Earth unlikely. A small solar flare effect (sfe) was observed in the rapid magnetograms of several stations.[6] However, the quiet geomagnetic conditions on 1982 June 3 provide no evidence for changes in the cutoff energies over Europe that are large enough to produce the observed enhancements.

The cosmic-ray intensity increases observed at Jungfraujoch, Lomnicky Stit and Rome are most simply explained by a transient flux of solar neutrons, incident on the Earth's atmosphere, with energies above 300 MeV (the threshold for producing a response in these monitors). Only the European neutron monitors had a nearly optimum response to direct solar neutrons, because of the time of the event. Furthermore, the observations at Jungfraujoch and Lomnicky Stit in the time interval 1145–1150 UT enable us to estimate the attenuation length of the secondary radiation in the atmosphere producing the excess count rate. The value obtained, 100 ± 8 g cm^{-2}, is in contrast to the attenuation length of 140 ± 10 g cm^{-2} characteristic for normal conditions. This latter value corresponds to the atmospheric attenuation length for secondary nucleons produced by primary cosmic rays above a cutoff energy of ~ 3.5 GeV, the local value for the two neutron monitors. Therefore, the average energy of the solar nucleons causing the flare enhancement must be less than for the cosmic-ray primaries above 3.5 GeV. This means that the atmospheric cascade, producing the excess count rate, was initiated by solar neutrons in the energy range 300 MeV–3.5 GeV.

[6] *Solar Geophysical Data.* 1982, No. 456, Part 1.

The presence of lower energy solar neutrons, >100 MeV, at the Earth in this event can be also established by the measurements of the *SMM* GRS. The high-energy detector, HEM, in the *SMM* GRS, described in Forrest *et al.* (1980), consists of seven 7.6 cm × 7.6 cm NaI elements and a single 25 cm × 7.5 cm CsI element, and records energy-loss events in all elements between 10 MeV and 100 MeV. The energy-loss distributions in the *SMM* high-energy detector were determined for all phases of the flare and compared with Monte Carlo calculations (Cooper *et al.* 1985), which are used to determine the GRS response to γ-rays (>10 MeV) and neutrons (>50 MeV). The Monte Carlo calculations predict that energy-loss events due to high-energy neutrons should be confined to individual detector elements rather than to simultaneous losses in both NaI and CsI. On the other hand, only γ-rays with energies greater than 50 MeV can produce a significant fraction of "mixed" or "shower" events; that is, energy loss in both the NaI and CsI detector elements (Forrest *et al.* 1987). Using this technique to identify the GRS neutron counts, Forrest *et al.* (1985) and Chupp *et al.* (1985) have demonstrated that in the delayed phase of the event the GRS was responding to a combination of photons and neutrons. Also, an analysis of the energy-loss distributions in the GRS HEM during the impulsive phase of this event indicates that γ-rays from the decay of π^0 mesons were detected (Forrest *et al.* 1985, 1987). The production of pions, which is accompanied (on average) by neutrons, has an energy threshold of ~ 290 MeV for p-p and ~ 180 MeV for p-α interactions, giving, therefore, a lower limit to the maximum energy of the particles accelerated at the Sun. Thus, if in the impulsive phase of this event both high-energy neutrons and γ-rays are produced by photons, the neutron energies must extend above 300 MeV.

Further satellite evidence for the arrival of neutrons at the Earth in this event is given by Evenson, Meyer, and Pyle (1983), who observed energetic protons (10–150 MeV) at the *ISEE 3* and *IMP 8* spacecrafts which they interpret as the decay products of neutrons generated in the solar flare. The neutrons emitted from the east limb flare site which are above the local horizon and which decay, at interplanetary field lines well connected to the spacecraft, give protons of approximately the same energy as the neutrons, which in turn are trapped by the field and can be efficiently detected.

Altogether, three independent observational techniques have provided direct evidence that energetic neutrons, reaching the Earth, were produced in the 1982 June 3 event.

IV. METHOD OF ANALYSIS

In general, the flux of neutrons from the Sun, measured at the Earth, at a time, t, is given by

$$F_n(t) = (D^{-2})q'(E_n, t_s)dE_n/dt_n\, P_s(E_n) \text{ (neutrons cm}^{-2}\text{ s}^{-1}), \quad (1)$$

where D is the Earth-Sun distance, E_n is the kinetic energy of the neutron, uniquely defined by $t_n = t - t_s$, the transit time of the neutron to the Earth, through the neutron velocity $\beta_n = Dc^{-1}(t - t_s)^{-1}$, c being the velocity of light. The quantity $q'(E_n, t_s)$ is the differential neutron emissivity spectrum for neutrons emitted from the Sun at time t_s and directed into a unit solid angle toward the Earth and is measured in units of (neutrons MeV^{-1} sr^{-1}). The derivative dE_n/dt_n is the neutron energy-time dispersion relation given by Lingenfelter and Ramaty (1967) and $P_s(E_n)$ is the survival probability for a neutron to reach the Earth before decay, both quantities dependent only on the neutron kinetic energy. Equation (1)

shows that if $q'(E_n, t_s)$ is nonzero only for one time, $t_s = t_0$, then neutrons arriving at 1 AU at time, t, will be monoenergetic and the flux time history is dependent only on the production energy spectrum. This is called the δ-function production model. Equation (1) also shows that if $q'(E_n, t_s)$ is nonzero over a finite time interval, then the neutron flux at $F_n(t)$, at any time t, will include a band of energies, each produced on the Sun at a different time t_s. In this case, neutron detectors with good energy resolution would be needed to separate the energy and time dependence of $q'(E_n, t_s)$.

The first observation of solar neutrons at the Earth on 1980 June 21 fits the δ-function neutron production model in which "time of flight" of a neutron to the Earth gives its energy directly. In this case it was possible to determine the neutron spectrum emitted from the Sun with observations from the *SMM* GRS even though this detector does not have good energy resolution (Chupp *et al.* 1982; Ramaty *et al.* 1983). However, in the present case it is not possible to use this model. To demonstrate this point we shall refer to the basic features of the GRS rates shown in Figure 1, evident in the time history of the curve for the greater than 25 MeV signal, as the impulsive emission 1143–1144 UT, and the delayed or time extended emission from ~1144 to 1204 UT, after which time the satellite entered into eclipse. First, the Jungfraujoch neutron monitor data cannot be explained by a δ-function model, since the excess count rate in this instrument extends over 11 minutes (Debrunner *et al.* 1983). A single burst of neutrons produced during the impulsive emission would have produced a neutron monitor enhancement lasting less than 5 minutes after the arrival of the first photons. Second, a detailed analysis of the GRS data also gives direct evidence for extended production of π^0 mesons, and therefore neutrons, during both the impulsive and extended emissions in the event. This analysis, described in a separate paper (Forrest *et al.* 1987), provides the basis for a neutron production time history at the Sun.

In addition to the evidence for a time-extended production of neutrons at the Sun, we must also consider the possibility that the neutron spectrum may be evolving with time. In an early interpretation of this event, Murphy and Ramaty (1985) suggested that most of the *SMM* GRS emissions could be explained by a proton Bessel function spectrum with a parameter $\alpha T = 0.04$ interacting in the solar atmosphere at the beginning of the event corresponding to ~1143–1144 UT. It was also suggested by these authors that a harder proton spectrum, producing enhanced neutral and charged pions, would be necessary to explain the harder γ-ray continuum later in the event (Fig. 1) and also the delayed 0.511 MeV annihilation γ-rays reported by Share *et al.* (1983). Therefore, in order to interpret the combined sets of neutron data from this event, one should, in principle, allow the impulsive and extended emission to have different spectral shapes. In this analysis of the neutron data alone, the assumption of different neutron production spectra during impulsive and extended emission periods would require numerous free parameters. Therefore, in the first interpretation of these data, we feel it is appropriate to use models with the smallest number of parameters. To see how well the simplest models fit the neutron data, we first constrain the time-averaged neutron spectral shapes in a way that is *independent of the neutron production time profile.* We then later test these allowed neutron spectral shapes against the full GRS and Jungfraujoch data sets. This test will use the observed pion γ-ray time history as representing the time history of the high-energy neutron (>50 MeV) production and assumes that the spectral forms are the same during both emissions, but we later also consider the observational effect of a time evolution of spectral forms.

To determine the time-averaged neutron emissivity spectra which are allowed we use the ratio of the time integrated counts from the two detectors. Since the maximum neutron detection sensitivities of the two detectors occur at considerably different energies, as shown in Figure 2, we find this ratio a unique discriminator of allowed spectra. Over the 11 minute interval from 1144 to 1145 UT, the Jungfraujoch neutron monitor recorded 3261 ± 415 counts, while from 1146 UT to near spacecraft sunset at ~1204 UT the GRS recorded 9055 ± 250 counts. This gives a Jungfraujoch to GRS total count ratio of 0.36 ± 0.05, where the error is 1 σ based on count statistics only. We have tested this observed ratio against that predicted using the following spectral functional forms for the neutron spectrum:

$$\text{Case a:} \quad q(E_n) \propto E_n^{-s}, \quad E_n \le E_c ;$$
$$q(E_n) \equiv 0, \quad E_n \ge E_c .$$
$$\text{Case b:} \quad q(E_n) \propto E_n^{3/8} \exp\left[-(E_n/3.26\phi^2)^{1/4}\right] .$$
$$\text{Case c:} \quad q(E_n) \propto \exp\left(-E_n/E_0\right) .$$

Similar functional forms have been used by McGuire and von Rosenvinge (1984) and others to describe the spectra of charged energetic solar particles in space. Each form, in general, has a different degree of curvature which depends on the spectral parameters s, ϕ, and E_0. We use these forms for mathematical convenience and also recognize that the proton and neutron spectral shapes are closely related. Since the

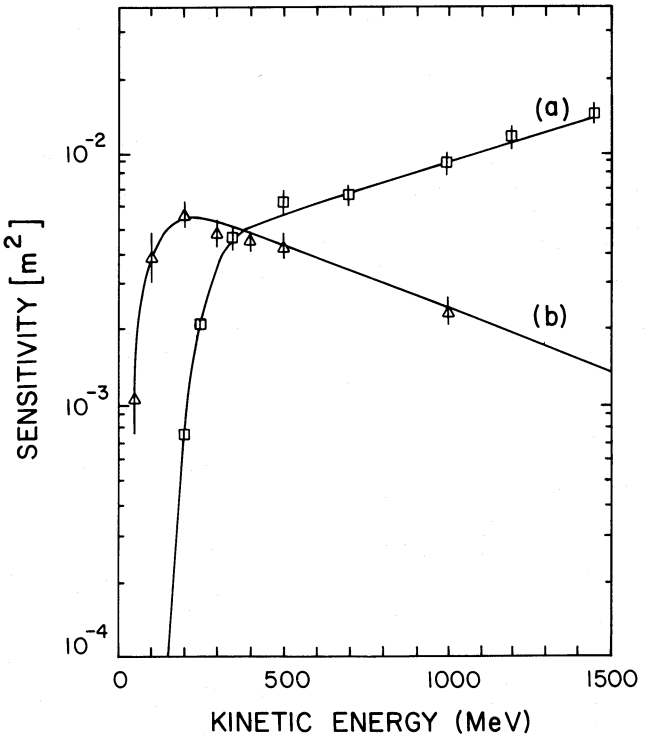

FIG. 2.—Nominal sensitivity functions for a standard IGY neutron monitor at 498.0 mm Hg atmospheric pressure for primary neutrons incident at the top of the atmosphere with a zenith angle of 25° (*a*) and for the *SMM* GRS (*b*).

power-law form, case a, with small s, can produce the hardest spectral shape and because of the very large Jungfraujoch sensitivity at high neutron energies, we include a cutoff energy E_c which may represent an end point in the acceleration process. The functional form, case b, is the same as the asymptotic limit for a Bessel function of the second kind, used to describe the protons resulting from a stochastic acceleration process (Ramaty 1986; Forman, Ramaty, and Zweibel 1986). Here the neutron spectral parameter, ϕ, replaces the proton spectral parameter αT.

The predicted Jungfraujoch neutron monitor to GRS count ratio was evaluated using equation (1), and the neutron monitor (Debrunner *et al.* 1983) and GRS (Cooper *et al.* 1985) sensitivities shown in Figure 2. The results are shown in Figures 3*a*–3*c*, where for each of the three spectral forms, the predicted count ratio is plotted versus the appropriate spectral parameter with a range of spectral parameter values for each case. Also shown in Figure 3, in the shaded band, is the range of values for the measured count ratio (0.31–0.41) determined from a variation of $\pm 1\ \sigma$ about the mean value as discussed above. The range of spectral parameter values allowed by the combined Jungfraujoch neutron monitor and GRS counts, for each spectral form, are bounded by the intersections of the predicted curves and the upper and lower values for the measured counts ratio. The predicted curves are based on the currently known nominal instrument sensitivities. Clearly the combined Jungfraujoch and GRS data strongly constrain the allowable spectral shape parameters for all three functional forms. The effect of the Jungfraujoch neutron monitor response at very high energies is clearly evident in the power-law ratio curve, but, as we shall show, other information can be used to investigate the limitations on the cutoff energy, E_c. It is important to note that the constraints shown in Figure 3 pertain to a "time-averaged neutron spectrum" and in this sense are independent of time evolution of the neutron spectrum produced in this flare. We next take into account the time-extended production of neutrons.

Forrest *et al.* (1987) show that the GRS high-energy counts (>10 MeV) during the impulsive emission are due to a mixture of photons from primary electron bremsstrahlung (>10 MeV) and a photon component resulting from π^0 meson decay and π^+ meson decay electron bremsstrahlung. During the extended emission, the events are due to a mixture of photons of only mesonic origin and high-energy neutrons. Photons of meson origin require proton energies of greater than 300 MeV for interactions with protons and 180 MeV for interactions with helium nuclei. Because the high-energy protons also produce high-energy neutrons, on average, we directly relate the time dependence of the neutron production at the Sun to the photon flux from meson decay, as represented by Figure 4*a*. By subtracting all of the photon contributions from the total GRS high-energy count rate we obtain the GRS neutron count rate shown as a histogram in Figure 4*b*. This unfolding procedure uses our Monte Carlo estimate of the GRS sensitivity to high-energy γ-rays and neutrons (Cooper *et al.* 1985) and is described in detail in Forrest *et al.* (1987). As discussed there, the actual number of counts attributed to meson decay photons, in Figure 4*a*, especially during the impulsive emission, is sensitive to assumptions about the actual shape of the pion decay γ-ray spectrum (Forrest *et al.* 1987) which, of course, depends on the unknown primary proton spectrum and the interaction geometry.

For the case of time-extended production of neutrons we

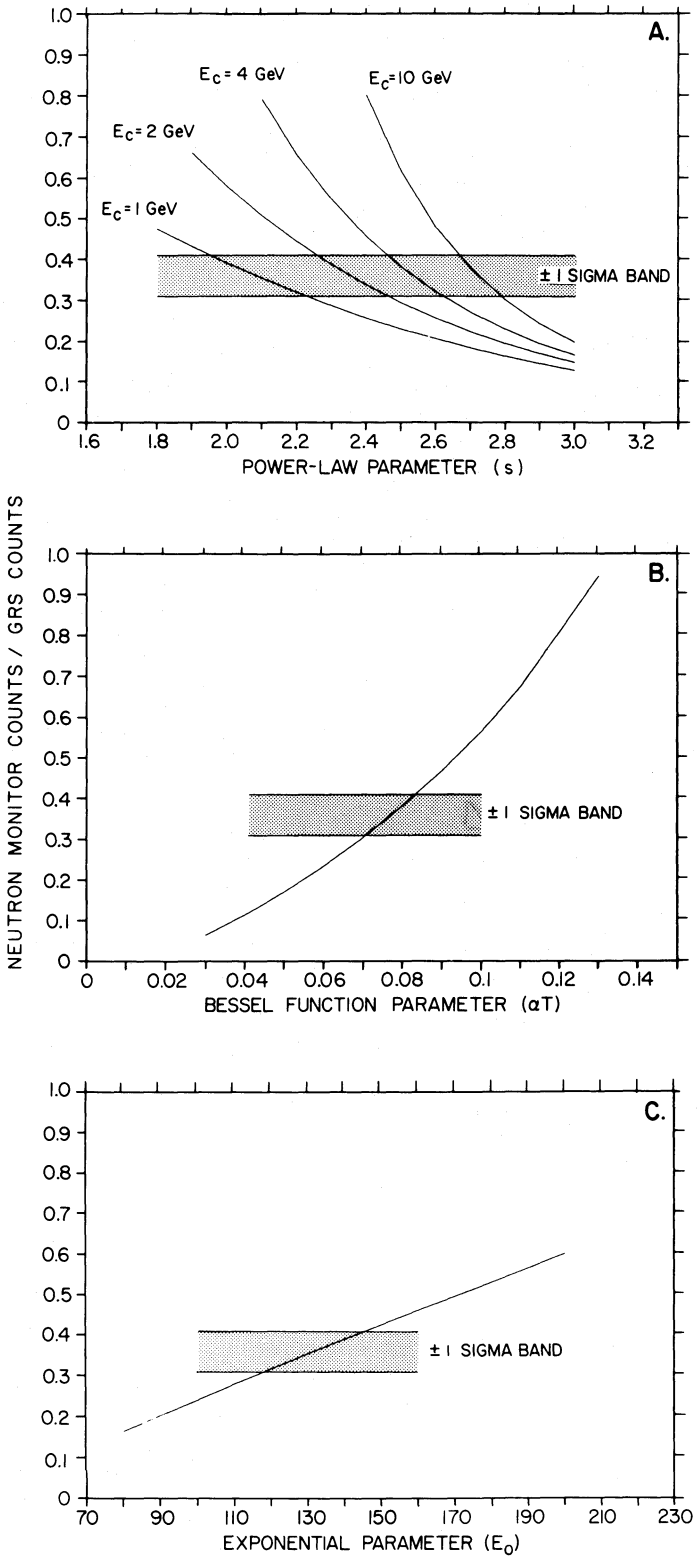

FIG. 3.—Curves show the ratio of the total predicted Jungfraujoch neutron monitor counts to the total GRS neutron counts plotted vs. the spectral parameter for the spectral forms (*a*) power law, (*b*) Bessel function, and (*c*) exponential. Shaded band shows the $\pm 1\ \sigma$ range of observed values of the ratio. Calculated curves use the detector sensitivities shown in Fig. 2 convolved with a given predicted neutron flux at the Earth and integrated from 50 MeV to ∞.

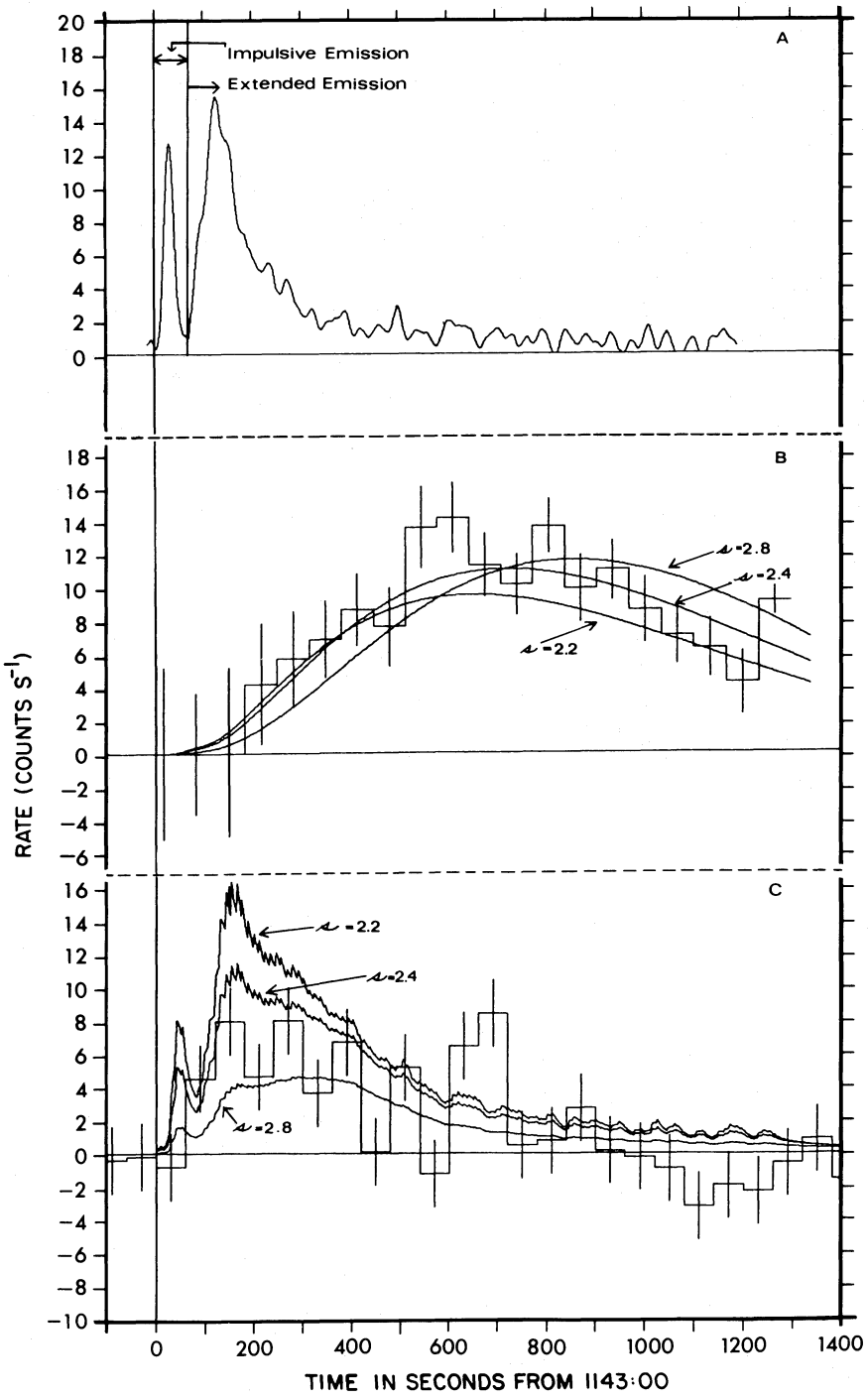

FIG. 4.—(*a*) Neutron production time histories at the Sun represented by the photon flux from meson decay. Separate production time histories are shown for the impulsive and extended emission. Data are smoothed to suppress statistical fluctuations. (*b*) Histogram gives the GRS neutron count rate averaged over 65.5 s intervals. The error bars are 1 σ based only on the observed count statistics. The three curves represent the best common fits for the predicted instantaneous GRS neutron count rates for power-law neutron spectra of the form, E_n^{-s}, with the corresponding exponents $s = 2.2$, 2.4, and 2.8 labeled on each curve. In all cases, the neutron spectra were truncated at 4 GeV. (*c*) Histogram gives the Jungfraujoch neutron monitor count rate averaged over 1 minute intervals. Error bars are 1 σ based on the observed count statistics. The three curves represent the best common fits for the predicted instantaneous neutron monitor count rates for power-law neutron spectra of the form, E_n^{-s}, with the corresponding exponents $s = 2.2$, 2.4, and 2.8 labeled on each curve. In all cases, the neutron spectra were truncated at 4 GeV as in Fig. 4*b*.

calculate predicted count rates of the GRS and the Jungfraujoch neutron monitor as a function of time and compare with the observed count rates. In our model testing we have assumed that the solar neutron emissivity spectrum $q'(E_n, t_s)$, in equation (1), is separable into a product of factors which depend separately on production time t_s and neutron energy, E_n. The former term, $f(t_s)$, is proportional to the pion γ-ray time history as discussed above and given in Figure 4*a*, and the second term is one of the neutron spectrum functional forms, $q(E_n)$, also given above.

The calculation proceeds as follows: We express the instantaneous count rate for either detector, for time-extended neutron production at the Sun by summing δ-function contributions from each successive 2 s time interval throughout the production phase at the Sun identified by the production time, t_s, using equation (1). Because of the relationship between neutron energy and transit time to the Earth, a given production time history, for a particular spectral form, will produce a particular form for the neutron spectrum versus time at the Earth, and, conversely, a given neutron spectrum at the Earth will imply a particular emission time history at the Sun. Since the GRS and Jungfraujoch neutron monitor have their peak sensitivities at greatly differing energies (Fig. 2), the combined data set can test differing assumptions about the production time history and neutron emissivity at the Sun. In the present analysis, we test spectra produced by an impulsive and a time-extended production model at the Sun. Previous tests using a δ-function production model alone do not give good fits to the *combined* GRS and Jungfraujoch neutron monitor data (Chupp *et al.* 1985). It should be noted that the energy-time dispersion relation, dE_n/dt_n, in equation (1), becomes a very significant factor at GeV energies where the Jungfraujoch neutron monitor has increasingly higher sensitivity. Numerical integrations giving the count rate time history for each detector have been carried out for a suitable distribution of time intervals throughout the event. A normalization constant, K, and hence absolute count-rate time distribution is then obtained for each production spectrum by using a χ^2 minimization procedure, *involving all data points for both instruments.* The time-integrated directional solar neutron emissivity, at the Sun in the direction of the Earth is then

$$Q(\text{neutrons MeV}^{-1}\ \text{sr}^{-1}) = \sum_{t_s} q'(E_n, t_s) = K \sum_{t_s} f(t_s) q(E_n)\,, \qquad (2)$$

where the summation is taken over the full production interval shown in Figure 4*a*. This procedure was carried out using several of spectral parameters for each spectral form within the ranges shown in Figure 3.

We discuss, in the next section, the comparison of the absolute count rate time distributions, predicted for each spectral form with observed count rates recorded in each instrument. Tests for sharp cutoffs or truncation near GeV energies for a particular spectrum and a study of the effect of the time evolution of the neutron spectrum at the Sun are also discussed.

V. RESULTS AND DISCUSSION

Examples of common fits to the count rates of the *SMM* GRS and the Jungfraujoch neutron monitor for several power-law spectra are shown in Figures 4*b* and 4*c*. The solid curves give the predicted instantaneous count rates for the spectral exponents $s = 2.2$, 2.4, and 2.8 to compare with the observed GRS and neutron monitor average rates also shown by histograms in Figures 4*b* and 4*c*, respectively. All neutron spectra used were cut off at $E_c = 4$ GeV. This is near the maximum energy permitted by the neutron monitor observations for a power-law spectral form (see below). A visual inspection of the GRS data and the model results shown in Figure 4*b* indicate generally acceptable fits for all three power-law spectral indices. The GRS contribution to the total $\chi^2_{\min}$ is $\chi^2/\text{dof} = 2.6$, 1.3, and 1.9, for $s = 2.2$, 2.4, and 2.8, respectively, for 17 degrees of freedom. This indicates that the spectral index 2.4 is preferred. Note that the low *SMM* GRS sensitivity at high neutron energies, E_n (see Fig. 2), results in a smooth temporal response. From inspection of Figure 4*c* it follows that only $s = 2.4$ leads to a visually adequate fit to the neutron monitor data. The resulting neutron monitor contribution to the total $\chi^2_{\min}$ is $\chi^2/\text{dof} = 3.1$ for 13 degrees of freedom.

The relatively poor agreement for the neutron monitor is due, in part, to the predicted peak in the count rate during the time interval 1143–1144 UT, whose amplitude is increasing with decreasing s, or increasing truncation energy E_c (see Fig. 7*b*). The fact that this predicted peak at the onset of the event has not been observed by the Jungfraujoch neutron monitor indicates that the neutron spectrum, at the Sun, during the impulsive emission could have been softer than the neutron spectrum during the extended emission. We believe, however, that the measurements do not allow determination of the free parameters of an emission model with two spectra in a conclusive way, and we therefore restrict the present analysis to a model with only one spectrum, as already discussed previously. A second cause of the relatively poor agreement between the experimental and theoretical data is the complex time structure in the neutron monitor count rate in the time interval 1150–1155 UT, which is not reflected by the calculated results. If the spikes in the Jungfraujoch neutron monitor count rate, between 1151 and 1152 UT and 1153 and 1155 UT, respectively, are due to neutrons with energies greater than 1 GeV, the Lomnicky Stit neutron monitor should have also measured an enhanced count rate in the interval 1150–1155 UT. If, on the other hand, the spikes observed at Jungfraujoch were caused by neutrons with energies between 300 and 500 MeV, increases of the count rate should have been detected by the *SMM* GRS. At present we are not able to explain the fine structure of the time history in all the measurements.

Uncertainties in the neutron sensitivity curves for the GRS and the neutron monitor can, of course, have an effect on the spectral forms the combined data sets allow. The error bars plotted in Figure 2 account for a 10% uncertainty of each value due to statistical fluctuations in the Monte Carlo simulation process and to uncertainties in the energy dependence of the parameters used in the simulations. However, due to uncertainties in the common neutron yield function for primary protons, used as a reference to normalize the yield function for primary neutrons, the latter is considered to be reliable only within a factor of 0.5–2 (see, e.g., Flückiger 1977). All calculations in this paper use the nominal sensitivity values given in Figure 2. We find acceptable fits for the power-law spectral form for $2.2 < s < 2.8$ with the best fit provided by $s = 2.4$ with an upper energy cutoff somewhat below 4 GeV.

Examples of common Bessel function spectra fits to the count rates of the two instruments are shown in Figures 5*a* and 5*b*, again using the neutron production function at the Sun shown in Figure 4*a*. Since this spectral form falls off naturally at the high energies, no cutoff is needed for the range of param-

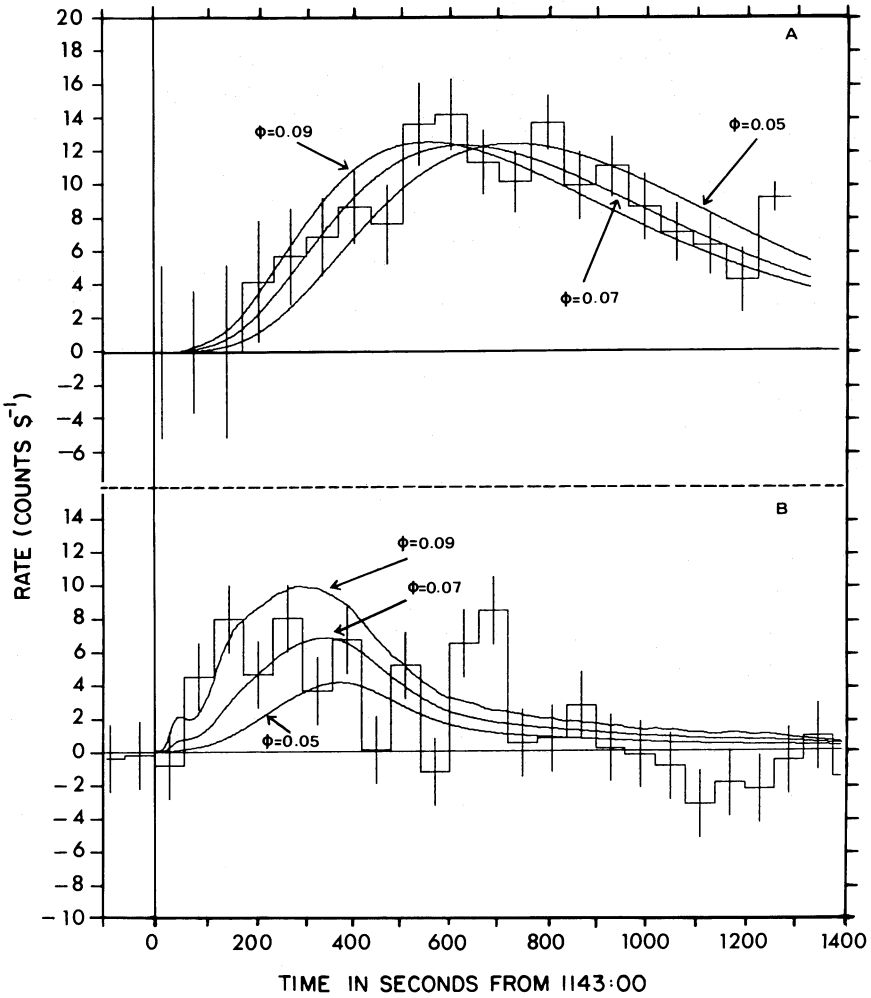

FIG. 5.—(*a*) Histogram gives the GRS neutron count rate averaged over 65.5 s intervals. Error bars are 1 σ based only on the observed count statistics. The three curves represent the best common fits for the predicted instantaneous GRS neutron count rates for Bessel function neutron spectra of the form $E_n^{3/8} \exp [-(E_n/3.3\phi^2)^{1/4}]$, with $\phi = 0.09$, 0.07, and 0.05 as shown by each curve. (*b*) Histogram gives the Jungfraujoch neutron monitor count rate averaged over 1 minute intervals. Error bars are 1 σ based on the observed count statistics. The three curves represent the best common fits for the predicted instantaneous neutron monitor count rates for Bessel function neutron spectra with the parameters $\phi = 0.09$, 0.07, and 0.05 as in Fig. 5*a*.

eters considered. The parameter $\phi = 0.07$ gives the best overall fit with the reduced χ^2/dof contributions for the GRS and neutron monitor of 1.6 and 2.8 for 18 and 14 degrees of freedom, respectively. The large value of χ^2 for the neutron monitor is due to the large variation in the count rate in the time interval 1150–1155 UT as in the case of the power-law spectrum discussed previously. The slower rise with time of the Bessel function count rate predictions give an additional substantial contribution to χ^2 in the first three minutes.

In the case of the exponential energy spectral form we found that parameter values in the range $120 < E_0(\text{MeV}) < 145$ satisfied the constraint required by the ratio of Jungfraujoch neutron monitor counts to the GRS counts as shown in Figure 3. However, when imposing the requirement to satisfy measured time histories we find a form with a single value of E_0 does not give a good fit. This is illustrated in Figures 6*a* and 6*b* which gives the predicted rates for each detector using $E_0 =$ 130 MeV and for which the values of χ^2/dof are 4.3 and 7.9 for the GRS and the neutron monitor, respectively.

As already seen, power-law neutron spectra require a high-energy cutoff in order to explain the Jungfraujoch neutron monitor count rate at the beginning of the event. An investigation of the effect of a cutoff, or truncation, of a spectral form at energies between 1 GeV and 10 GeV was performed in the course of determining best fits. Examples of the results are shown in Figure 7 for the power-law spectrum with spectral parameters $s = 2.4$. A visual inspection of Figure 7 and a χ^2 test rejects cutoffs for $E \geq 6$ GeV. Using the results shown in Figures 4 and 7, we conclude that the best fit found for the power law is with parameter $s = 2.4$ and $E_c = 2$ GeV. Neutrons with energies ≥ 1 GeV had to be present to cause the increase of the Jungfraujoch neutron monitor count rate in the time interval 1144–1145 UT. At this point it is appropriate to discuss the possibility of a time delay between the production of high-energy γ-rays and neutrons. A delay is possible since the production time history shown in Figure 4*a* is due to the portion of the proton spectrum above $\sim$300 MeV, but the high-energy neutrons necessary to give the early JFNM response are produced by higher-energy protons that could take longer to peak in intensity than those producing the pions. By inspection of Figure 4*a*, it can be seen that during the impulsive emission, the pion γ-ray pulse envelope is approx-

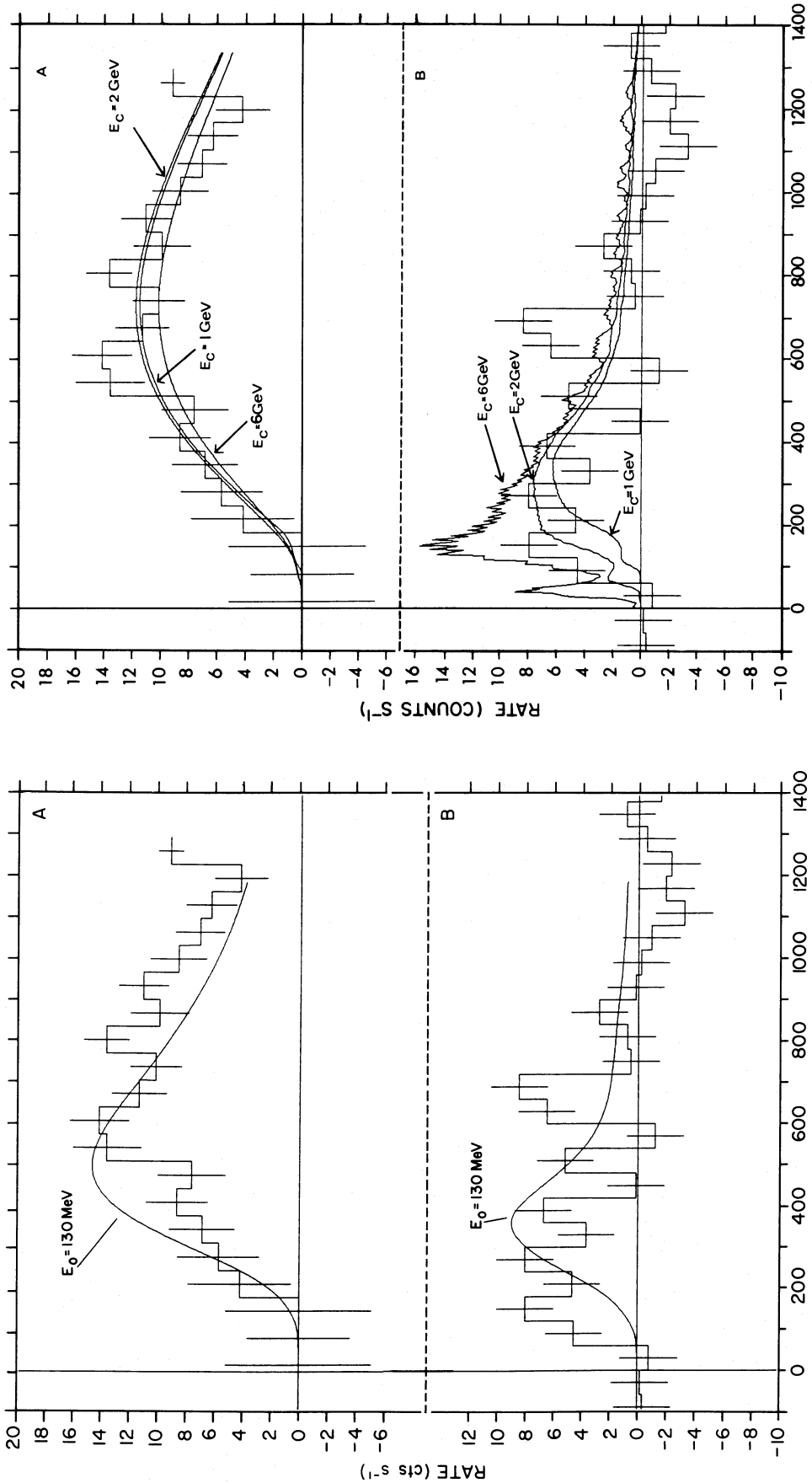

FIG. 6.—(*a*) Histogram gives the GRS neutron count rate averaged over 65.5 s intervals. Error bars are 1 σ based only on the observed count rate. The continuous curve shows a fit for the predicted instantaneous GRS neutron count rate for an exponential energy spectrum of the form, $\exp(-E_n/130\ \mathrm{MeV})$ as discussed in the text. (*b*) Histogram gives the Jungfraujoch neutron monitor count rate averaged over 1 minute intervals. Error bars are 1 σ based only on the observed count rate. The continuous curve shows a fit for the predicted instantaneous neutron monitor count rate for the exponential energy spectrum as discussed in the text and shown in Fig. 6*a*.

FIG. 7.—(*a*) Histogram gives the GRS neutron count rate averaged over 65.5 s intervals. Error bars are 1 σ, based only on observed count statistics. The three curves represent the GRS count rate for the single neutron power-law energy spectrum of form $E^{-2.4}$ when truncated at an energy E_c = 1, 2, or 6 GeV. (*b*) Histogram gives the Jungfraujoch neutron monitor count rate averaged over 1 minute intervals. Error bars are 1 σ, based only on observed count statistics. The three curves represent the neutron monitor count rate for the single power-law neutron energy spectrum of form $E^{-2.4}$ when truncated at an energy E_c = 1, 2, or 6 GeV as in Fig. 7*a*.

imately symmetric with a half-width of ~16 s. If we consider the decay of the pion γ-ray time profile it is clear that the interaction time of particles producing the pions and/or the ionization loss time scale of these ions must be *less* than the half-width of the first pion γ-ray pulse. Therefore, neutron production during impulsive emission could not be delayed by more than ~16 s. Suppose, however, that we go to the extreme and argue that there is negligible production of high-energy neutrons in the impulsive emission, then a much higher neutron energy will be required to give the early neutron monitor response than if there is neutron production during the impulsive emission. In addition, the cutoff of the neutron spectrum would be allowed to higher energies (see Fig. 7*b*). Therefore, by comparing the neutron monitor data and the GRS data of the photons from meson decay at the onset of the event it also follows that the first GeV protons, producing the GeV neutrons, appeared at the Sun with a delay of, at most, ~16 s with respect to the first interacting (>300 MeV) protons.

Our method of analysis gives us directly the total absolute neutron emissivity spectrum at the Sun, Q (neutrons MeV^{-1} sr^{-1}), from equation (2). For the case of the power-law form we find

$$Q = 7.4 \times 10^{31} E_n^{-2.4}, \quad 100 < E_n \leq 2000, \tag{3}$$

for the Bessel function form,

$$Q = 1.4 \times 10^{30} E_n^{3/8} \exp\left[-(E_n/0.016)^{1/4}\right], \quad E_n > 100, \tag{4}$$

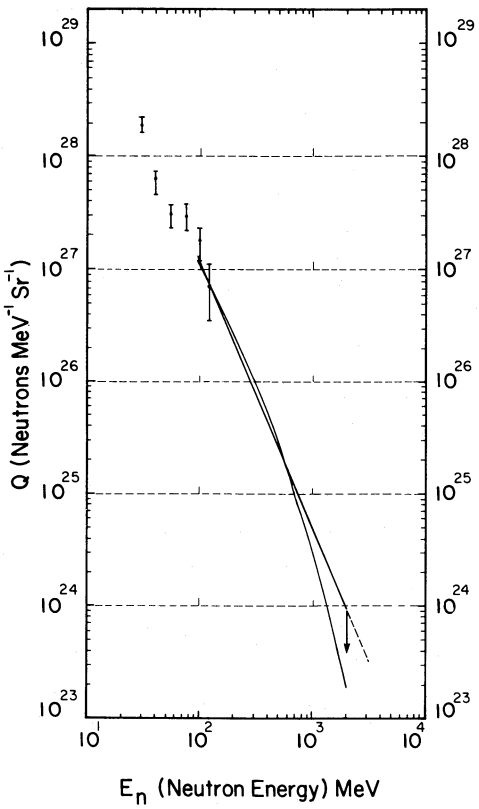

FIG. 8.—Time-integrated directional solar neutron emissivity spectrum is shown for the best-fit power-law and Bessel function neutron spectral forms with parameters $s = 2.4$ and $\phi = 0.07$, respectively. Data points from the neutron decay proton observations (Evenson *et al.* 1983) are also shown (see text).

and for the exponential form,

$$Q = 1.4 \times 10^{27} \exp\left[-(E_n/130)\right], \quad E_n > 100, \tag{5}$$

where E_n is given in MeV in all cases. These quantities give directly the emissivity spectrum in the direction of the Earth as determined from the GRS and the neutron monitor data. The first two spectra are plotted in Figure 8 and represent a range of acceptable fits to the combined data sets. These fits agree well with the *total* neutron emissivity spectrum above 100 MeV, which we previously presented (Chupp *et al.* 1984), based on preliminary *SMM* GRS data and JFNM data, assuming a δ-function neutron emission from the Sun, even though we do not now consider this a valid production model for this event.

The *SMM* GRS data do not permit an extension of the spectra below ~100 MeV because of the rapidly falling instrument sensitivity and the fact that the satellite is near eclipse. We can provide comparative data points for neutrons at lower energies, which escape the Sun, from the observation of neutron decay protons. We use the results of Evenson, Kroeger, and Meyer (1985) which give the total neutron emissivity spectrum for isotropic emission and convert them to appropriate units shown in Figure 8. An examination of the figure shows that the emissivity spectra deduced above 100 MeV are in good agreement with the lower points derived. The total number of neutrons above 100 MeV for all three of the spectral forms considered is $\sim 8 \times 10^{28}$ neutrons sr^{-1}; however, the exponential form does not give a reasonable fit to the observed time history. The contribution to the total neutron emissivity, in all cases, comes predominantly (>80%) from the extended emission, as can be seen from examination of Figure 4*a*. This is a direct contradiction to the δ-function model, which assumed that a 100% of the neutrons were produced during the impulsive emission. It seems that the *time integrated neutron spectrum* (>100 MeV) is not particularly sensitive to the details of the production models used thus far.

As we have discussed in § IV, there is evidence to suggest that the production spectrum of the high-energy neutrons has evolved in time. We have considered the observational consequences of this possibility, following the approach of Murphy *et al.* (1986). Our analysis demonstrates that it is possible to find different spectral forms during the impulsive and extended emissions which give reasonable fits to the combined GRS and Jungfraujoch neutron data. It is clear, however, that in our analysis the large number of parameters necessary for such emission models cannot be adequately constrained, based on our experimental data. Besides our model of production of neutrons with constant spectral shape throughout the impulsive and extended emissions, we can consider two other extreme models involving the fewest parameters: (1) neutron production only during the impulsive emission, and (2) neutron production only during the extended emission. In the first case, Murphy and Ramaty (1985) at the Graz COSPAR Conference have shown that this is essentially a δ-function model, even if time extended production for ~1–2 minutes is considered. We find, however, that this does not give an adequate fit to the combined JFNM, GRS data sets, particularly because the neutron monitor data requires time-extended production. In the second case the GRS data can be fitted reasonably well, but the initial rise of the neutron monitor is not fitted well unless the high-energy cutoff in the neutron spectrum is greatly increased. This only increases the requirement for the accelerator and furthermore ignores the pion γ-ray evidence for high-

energy neutron production during both the impulsive and extended emission. Further, the minimum parameter models, with no dramatic spectral time evolution, show that more than 80% of the neutrons above 100 MeV have been produced during the extended emission.

VI. CONCLUSIONS

For the solar neutron event on 1982 June 3, we have shown that the combined *SMM* GRS and Jungfraujoch neutron monitor data require a time-extended emission of neutrons at the Sun with energies of 100 MeV to ~ 2 GeV. Using a neutron production time history determined from the *SMM* GRS pion γ-ray data (and the currently known nominal instrument sensitivities), we have determined the solar neutron emissivity spectrum using neutron spectral forms with different degrees of curvature and assuming that the spectral form is constant throughout the impulsive and extended emission from the event. Our analysis shows that at energies between 2 and 4 GeV the spectrum must have a strong downward curvature or be truncated. The required curvature is introduced naturally by the Bessel function form for $0.05 < \phi < 0.09$. In the case of the power-law form with a spectral parameter $s \approx 2.4$, a truncation at an energy E_c is required in the range $2 < E_c < 4$ GeV. While the truncated power-law and Bessel function forms give acceptable fits to the observational data, only the power law can explain the rapid rise of the neutron monitor count rate. We find that the integrated emissivity of neutrons above $E_n >$ 100 MeV is strongly constrained at 8×10^{28} neutrons sr^{-1} and is essentially independent of neutron spectral shape. At neutron energies of ~ 100 MeV good agreement is found for both spectral forms with the observations of neutron decay protons (Evenson, Kroeger, and Meyer 1985).

The present analysis has been carried out by using the pion γ-ray intensity time history as a measure of the neutron production time profile at the Sun. This assumption means that $\sim 80\%$ of the neutrons with $E_n > 100$ MeV were produced in the extended phase of the event. Nevertheless, the production of pions and neutrons in the impulsive emission places strong constraints on the proton energies and the density of the region where the energetic secondaries were produced. In this phase, the pion γ-ray pulse envelope is approximately symmetric with a half-width of < 16 s (see Fig. 1), and the neutron production rate must also conform to this time history. (If we assume production of the first neutrons any later than this, for example at the time of the peak in the extended emission, we would not be able to explain the neutron monitor data; (cf. Figs. 4*a* and 4*c*). Since the production of neutrons of a given energy requires protons of somewhat higher energies, we can conclude that protons were accelerated to GeV energies with a time scale less than 16 s. Because of their good time correlation, the γ-ray temporal features shown in Figure 1 must be a result of the time scale of interactions of the impulsive injection of ions, into a target, which could span an energy range of ~ 10 MeV $< E_p < 3$ GeV. By considering the nuclear interaction loss time scale, Δt, in hydrogen, we can place a lower limit on the number density in the interaction region. For neutron production by relativistic protons in hydrogen, with a cross section $\sigma = 20$ mb, it is necessary for the target density to be $n > 16(\Delta t)^{-1}(16\ \sigma c)^{-1} > 16(\Delta t)^{-1}10^{14}$ cm^{-3}. It is also clear that the width of the acceleration pulse itself could be much shorter (Kane *et al.* 1986) than the minimum interaction time scale required by the duration of the first impulse in the *SMM* GRS data which is $\Delta t \approx 16$ s in the present case.

The angular distribution of the neutron emission in this event cannot be inferred from neutrons measured from a single observation point. On the other hand, the neutron decay proton observations themselves cannot differentiate between an isotropic emission pattern and one with an extreme anisotropy as represented by emission parallel only to the horizon at the flare site (Evenson, Kroeger, and Meyer 1985; Evenson 1986). More information on this important question may result from further analysis of all observations made on this event, from radio waves to high-energy γ-rays, together with the direct neutrons. Further work in progress will take into account this information, and in addition we will consider further the emission models in which the neutron energy spectrum changes with time.

Until now the production of GeV solar protons was evident only from the infrequent solar cosmic-ray ground-level events (GLEs) which occur with an average rate of ~ 1 yr^{-1}. The most energetic GLE on 1956 February 23 was due to protons with energies up to 30 GeV (Meyer, Parker, and Simpson 1956). It remains an intriguing problem to relate the spectrum of the protons producing the γ-rays and neutrons at the Sun to that of the solar energetic protons observed in interplanetary space and at the Earth (Chupp 1984; Debrunner *et al.* 1984).

The authors wish to thank Sally Cote, Christian Seymour, and Gudrun Sturzenegger for typing this manuscript. For the analysis assistance we thank Karen Dowd, Sabrina Kirwan, and Bao Li. We also thank Gaby Sebor and Marcus Schubnell for help in analysis of the Jungfraujoch neutron monitor data. We would like to single out with a special thanks Kenneth Levenson for his exceptional contribution to the data analysis of the *SMM* GRS and the Jungfraujoch neutron monitor data. We also wish to express our profound appreciation to Mary M. Chupp for her tireless editorial help, on three continents, during all phases, drafts, and the final execution of this paper. We also appreciate the constructive suggestions of the reviewer. This work was supported in part by NASA and the Air Force under contract NAS 5-28609 and grant NAG5-720 at the University of New Hampshire; NASA contract S.14513-D at the Naval Research Laboratory, contract 010K017ZA/WS/WRK 0275:4 at the Max-Planck Institut, FRG; and Swiss National Science Foundation Grant 2.632-0.85 at the University of Bern in Switzerland. Finally, we express our gratitude to G. Haerendel, director of the Max-Planck Institute for Extraterrestrial Physics, Garching, West Germany, for his support and hospitality during the completion of this paper.

REFERENCES

Alsmiller, R. G., and Boughner, R. T. 1968, *J. Geophys. Res.*, **73**, 4935.
Biermann, L., Haxel, O., and Schluter, A. 1951, *Zs. Naturforschung*, **6a**, 47.
Chupp, E. L. 1971, *Space Sci. Rev.*, **12**, 486.
———. 1982, in *Gamma-Ray Transient Astrophysical Phenomena*, ed. R. E. Lingenfelter, H. S. Hudson, D. M. Worrall (Dordrecht: Reidel), p. 363.
———. 1984, *Ann. Rev. Astr. Ap.*, **22**, 359.
Chupp, E. L., *et al.* 1982, *Ap. J.* (*Letters*), **263**, L95.
———. 1984, *Proc. 18th Internat. Cosmic Ray Conf.*, **10**, 344.
———. 1985, *Proc. 19th Internat. Cosmic Ray Conf.*, **4**, 126.
Cooper, J. F., *et al.* 1985, *Proc. 19th Internat. Cosmic Ray Conf.*, **5**, 474.
Debrunner, H., Flückiger, E., Chupp, E. L., and Forrest, D. J. 1983, *Proc. 18th Internat. Cosmic Ray Conf.*, **4**, 75.
Debrunner, H., Flückiger, E., Lockwood, J. A., and McGuire, R. E. 1984, *J. Geophys. Res.*, **89d**, 769.
Efimov, Yu. E., Kocharov, G. E., and Kudela, K. 1983, *Proc. 18th Internat. Cosmic Ray Conf.*, **10**, 276.
Evenson, P. 1986, private communication.
Evenson, P., Kroeger, R., and Meyer, P. 1985, *Proc. 19th Internat. Cosmic Ray Conf.*, **4**, 130.
Evenson, P., Meyer, P., and Pyle, K. R. 1983, *Ap. J.*, **274**, 875.
Evenson, P., Meyer, P., Yanagita, S., and Forrest, D. J. 1984, *Ap. J.*, **283**, 439.
Flückiger, E. 1977, *Proc. 15th Internat. Cosmic Ray Conf.*, **4**, 144.
Forman, M. A., Ramaty, R., and Zweibel, E. G. 1986, in *Physics of the Sun*, Vol. **2**, *The Acceleration and Propagation of Solar Flare Energetic Particles*, ed. Peter A. Sturrock (Dordrecht: Reidel), p. 249.
Forrest, D. J., and Chupp, E. L. 1969, *Solar Physics*, **6**, 339.
Forrest, D. J., *et al.* 1980, *Solar Phys.*, **65**, 15.
———. 1985, *Proc. 19th Internat. Cosmic Ray Conf.*, **4**, 146.
———. 1987, in preparation.
Kane, S. 1982, private communication.
Kane, S., Chupp, E. L., Forrest, D. J., Share, G. H., and Rieger, E. 1986, *Ap. J.* (*Letters*), **300**, L95.
Kirsch, E. 1973, *Solar Phys.*, **28**, 233.
Kocharov, G. E., and Mandzhavidze, N. Z. 1985, *Proc. 19th Internat. Cosmic Ray Conf.*, **4**, 150.
Kudela, S. 1983, private communication.
Lingenfelter, R. E., Flamm, E. J., Canfield, E. H., and Kellman, S. 1965, *J. Geophys. Res.*, **70**, 4077.
Lingenfelter, R. E., and Ramaty, R. 1967, in *High Energy Nuclear Reactions in Astrophysics*, ed. B. S. P. Shen (New York: Benjamin), p. 99.
McDonald, F. B., and Van Hollebeke, M. A. I. 1985, *Ap. J.* (*Letters*), **290**, L67.
McGuire, R. E., and von Rosenvinge, T. T. 1984, *Adv. Space Res.*, **4**, 117.
Meyer, P., Parker, E. N., and Simpson, J. A. 1956, *Phys. Rev.*, **104**, 768.
Murphy, R. J. 1985, Ph.D. thesis, University of Maryland.
Murphy, R. J., Dermer, G. D., and Ramaty, R. 1986, *Ap. J.*, in press.
Murphy, R. J., and Ramaty, R. 1985, *Adv. Space Res.*, **4**, 127.
Prince, T. A., Forrest, D. J., Chupp, E. L., Kanbach, G., and Share, G. H. 1983, *Proc. 18th Internat. Cosmic Ray Conf.*, **4**, 79.
Ramaty, R. 1986, in *Physics of the Sun*, Vol. **2**, *Nuclear Processes in Solar Flares*, ed. Peter A. Sturrock (Dordrecht: Reidel), p. 291.
Ramaty, R., Kozlovsky, B., and Lingenfelter, R. E. 1975, *Space Sci. Rev.*, **18**, 341.
Ramaty, R., Murphy, R. J., Kozlovsky, B., and Lingenfelter, R. E. 1983, *Ap. J.* (*Letters*), **273**, L41.
Roelof, E. 1966, *J. Geophys. Res.*, **71**, 5.
Rohrs, K. 1983, private communication.
Share, G. H., Chupp, E. L., Forrest, D. J., and Reiger, E. 1983, in *Positron and Electron Pairs in Astrophysics*, ed. M. L. Burns *et al.* (New York: AIP), p. 15.
Share, G. H., Forrest, D. J., Chupp, E. L., and Rieger, E. 1982, *Bull. AAS*, **14**, 875.
Shea, M. A., Smart, D. F., and Gentile, L. C. 1983, *Proc. 18th Internat. Cosmic Ray Conf.*, **3**, 411.
Simpson, J. A., and Uretz, R. B. 1953, *Phys. Rev.*, **90**, 44.
Zangrilli, N. 1983, private communication.

E. L. CHUPP, D. J. FORREST, and W. T. VESTRAND: University of New Hampshire, Durham, NH 03824

J. COOPER: California Institute of Technology, Division of Physics and Astronomy, Pasadena, CA 91125

H. DEBRUNNER, E. FLÜCKIGER, and F. GOLLIEZ: Physikalisches Institut der Universität Bern, 3012 Bern, Switzerland

G. KANBACH: Max-Planck Institut für Extraterrestrische Physik, 8046 Garching, West Germany

G. SHARE: E. O. Hulburt Center for Space Research, Naval Research Laboratory, Washington, DC 20375